# Interaction of S100A1 with the $Ca^{2+}$ Release Channel (Ryanodine Receptor) of Skeletal Muscle†

Susan Treves,*,‡ Erica Scutari,‡ Mylène Robert,§ Séverine Groh,§ Michela Ottolia,|| Gianfranco Prestipino,|| Michel Ronjat,§ and Francesco Zorzato‡

*Istituto di Patologia Generale, Università di Ferrara, Via Borsari 46, 44100 Ferrara, Italy, Laboratoire de Biophysique Molèculaire et Cellulaire, URA 520 du CNRS, CEA/CENG, Dèpartment de Biologie Molèculaire et Structurale, 17 rue des Martyrs, 38054 Grenoble Cèdex 9, France, and Istituto di Cibernetica e Biofisica, CNR, Via De Marini 6, 16149 Genova, Italy*

*Received January 23, 1997; Revised Manuscript Received July 2, 1997*⊗

ABSTRACT: In the present report we studied the interaction between the skeletal muscle ryanodine receptor and the ubiquitous S100A1 $Ca^{2+}$ binding protein. S100A1 did not affect equilibrium [$^3$H]ryanodine binding to purified rabbit skeletal muscle terminal cisternae at 100 $\mu$M free [$Ca^{2+}$]. At nanomolar free [$Ca^{2+}$], however, S100A1 activated by 40 ± 6.7% (mean ± SE, $n = 5$) the [$^3$H]ryanodine binding activity; the half-maximal concentration for stimulation of [$^3$H]ryanodine binding was approximately 70 nM, a value well below the estimated S100A1 concentration in skeletal muscle fibers. Scatchard analysis of [$^3$H]-ryanodine binding performed in the presence of 100 $\mu$M EGTA indicates that S100A1 increases the apparent affinity of the receptor for ryanodine ($K_d = 191$ vs 383 nM in the presence and in the absence of 100 nM S100A1, respectively). The effect of S100A1 was also tested on the single-channel gating properties of the purified ryanodine receptor after reconstitution into a lipid planar bilayer. Currents carried by purified ryanodine receptor channels were modulated by both *cis* $Ca^{2+}$ and ruthenium red. In the presence of nanomolar [$Ca^{2+}$], S100A1 activated the channel by increasing (6.0 ± 2.8)-fold (mean ± SE, $n = 3$) the normalized open probability. The interaction between S100A1 and the purified RYR was verified using the optical biosensor BIAcore: we show that the two proteins interact directly both at millimolar and at nanomolar calcium concentrations. We next mapped the regions of the skeletal muscle RYR involved in the interaction with S100A1 by performing ligand overlays on a panel RYR of fusion proteins in the presence of 100 nM S100A1. Our results indicate that the skeletal muscle RYR contains three potential S100A1 binding domains. Binding of S100A1 to the RYR fusion proteins occurred at both nanomolar and millimolar free [$Ca^{2+}$]. S100A1 binding domain 1 binds the ligand in the presence of 1 mM free [$Ca^{2+}$] or 1 mM EGTA. Maximal binding to S100A1#2 was achieved in the presence of 1 mM free [$Ca^{2+}$]. The S100A1#3 domain, which overlaps with calcium-dependent calmodulin binding domain 3 (CaM 3), exhibits weak and strong S100A1 binding activity in the presence of either millimolar or nanomolar $Ca^{2+}$, respectively. The interaction between S100A1 and the purified RYR complex was also investigated by affinity chromatography: in the presence of nanomolar $Ca^{2+}$, we observed binding of native RYR complex to S100A1-conjugated Sepharose. This interaction could be inhibited by the presence of RYR polypeptides encompassing S100A1 binding sites S100A1#1, S100A1#2, and S100A1#3.

The ryanodine receptor (RYR),[1] the $Ca^{2+}$ release channel of sarco(endo)plasmic reticulum, is a large tetrameric oligomer which forms a cation channel upon reconstitution in planar lipid bilayers (*1*, *2*). Three isoforms have been identified and characterized at the molecular level: type 1 appears to be skeletal muscle specific; type 2 is expressed in the heart, though it is also present in the cerebellum and to a lower extent in other regions of the brain; type 3 is present throughout the central nervous system and in other tissues (*3*). The primary structures of skeletal, cardiac, and brain ryanodine receptors have been obtained, and sequence analysis comparison has established an overall homology of approximately 60% among the three isoforms (*4*, *5*, *6*, *7*). Purification of the RYR from skeletal muscle yields a complex made up of four polypeptides of 565 kDa molecular mass which are associated with four FK506 binding proteins (FKBP12) with a stoichiometry ratio of 1:1 (*8*). Besides FKBP12, other proteins including calsequestrin, annexin VI, triadin, aldolase, calpain, and calmodulin have been reported to interact with the RYR tetramer and modify its function (for a review, see ref *2*). However, the exact functional relevance of such RYR-associated proteins has not been clearly established.

In the present report, we have investigated the capacity of S100A1, a member of the $Ca^{2+}$ binding protein family known as S100 (*9*, *10*), to interact with the rabbit skeletal muscle RYR. The S100 proteins have been reported to be

† This work was supported by grants from Telethon (Italy), Consiglio Nazionale delle Ricerche CT04, Ministero dell'Università e della Ricerca Scientifica e Tecnologica 40% and 60%, and Association Francaise contre les Myopathies.

* To whom correspondence should be addressed at the Institute of General Pathology, Via Borsari 46, 44100 Ferrara, Italy. Telephone: (Italy)-532-291-356. Fax: (Italy)-532-247-278.

‡ Università di Ferrara.

§ CEA/CENG.

|| CNR.

⊗ Abstract published in *Advance ACS Abstracts,* August 15, 1997.

[1] Abbreviations: RYR, ryanodine receptor; SR, sarcoplasmic reticulum; EGTA, [ethylenebis(oxyethylenenitrilo)]tetraacetic acid; HEPES, *N*-2-(hydroxyethyl)piperazine-*N*′-2-ethanesulfonic acid; Tris, tris(hydroxymethyl)aminomethane; SDS, sodium dodecyl sulfate; PAGE, polyacrylamide gel electrophoresis; TC, terminal cisternae; DTT, 1,4-dithio-L-threitol.

S0006-2960(97)00160-8 CCC: $14.00 

involved in numerous physiological functions, such as cell cycle progression, cell differentiation, and cytoskeleton-mediated interactions, though their role *in vivo* is far from clear; in this context, it should be mentioned that S100A1 has been reported to interact with protein domains capable of binding calmodulin (*11*). More than 10 different members belong to the S100 protein family (*8*); S100A1 is preferentially expressed in striated muscles and a small population of neurons. It has been found to associate with sarco(endo)-plasmic reticulum membranes and shown to stimulate $Ca^{2+}$-induced $Ca^{2+}$ release from skeletal muscle terminal cisternae (*12*, *13*). These observations prompted us to investigate whether S100A1 is able to interact with the RYR, and in particular with the regions capable of binding calmodulin. Here we show that S100A1 is capable of binding to RYR polypeptides defined by residues 1861−2155 (S100A1#1), 3774−3874 (S100A1#2), and 4425−4621 (S100A1#3). The most interesting and novel result reported in this study concerns the ability of the RYR to bind S100A1 in the presence of nanomolar $Ca^{2+}$. Such an interaction at free [$Ca^{2+}$] similar to those present in resting muscle causes an enhancement of the equilibrium binding of [$^3$H]ryanodine to the RYR by 40% ± 6.4% (mean ± SE, $n = 5$), and increases the normalized open probability of purified RYR channel reconstituted in the planar lipid bilayer. Half-maximal stimulation of [$^3$H]ryanodine binding occurred at 68 nM S100A1, a concentration well below the estimated concentration of S100A1 in skeletal muscle cells (*14*).

## MATERIALS AND METHODS

### *Materials*

S100A1 purified from bovine brain, anti-S100A1 Ab, and S100A1-conjugated Sepharose resin were invaluable and were a generous gift from Dr. J. Baudier, INSERM Unitè 244, DBMS-BRCE, CEN-G, Grenoble, France. S100A1 concentration was calculated spectrophotometrically assuming an absorption extinction coefficient of 18 000 $M^{-1}$ $cm^{-1}$ at 277 nm. We also used S100A1 (S-2650) from Sigma, St. Louis, MO; however, the protein content of the commercial preparation of S100A1 (S-2650) was extremely variable. Calmodulin was from Boehringer, Mannheim (catalog no. 651222). Anti-RYR polyclonal antibodies directed against the C-terminal region of the RYR protomer were prepared as previously described by Marty et al. (*15*).

### *Methods*

*Preparation of Sarcoplasmic Reticulum Fractions and Purified RYR*. Terminal cisternae were obtained from the white skeletal muscles of New Zealand 2.5−3 kg male rabbits as described by Saito et al. (*16*). Protein concentration was measured according to Lowry (*17*), using bovine serum albumin as standard. In order to obtain the junctional face membrane, terminal cisternae fractions were solubilized with Triton X-100 as described by Costello et al. (*18*). The rabbit skeletal muscle RYR was purified according to Lai et al. (*19*).

*Real Time Surface Plasmon Resonance Recording*. For real time plasmon resonance binding experiments, a BIAcore biosensor system (Pharmacia Biotech Inc.) was used. All experiments were performed at 25 °C as previously described by Zorzato et al. (*20*) except that S100A1 was directly coupled to the biosensor chip using the amino coupling kit (Pharmacia Biotech Inc.). Before use, the purified RYR was dialyzed overnight at 4 °C against a buffer containing 20 mM HEPES, pH 7.4, 150 mM KCl.

*DNA Manipulation and Production of Fusion Proteins*. DNA manipulations were carried out according to standard protocols as described in Maniatis et al. (*21*). To cover the entire RYR coding sequence, we constructed several fusion proteins; the details of the construction have been previously described (*22*, *23*).

*Indirect Immunoenzymatic Staining with Anti-S100A1 Ab*. Indirect immunoenzymatic staining of a Western blot of S100A1 and calmodulin was carried out as described by Menegazzi et al. (*23*).

*S100A1 Ligand Overlay*. S100A1 was labeled with activated digoxigenin according to the manufacturer's instructions (Boehringer, Mannheim, FRG). Overlays of Western blots of bacterial extracts were performed as previously described by Menegazzi et al. (*23*) except that the ligand was digoxigenin-labeled S100 (final concentration 100 nM). Overlays were performed either in the presence of 1 mM $Ca^{2+}$ or in the presence of 1 mM EGTA.

*Ryanodine Binding*. Briefly, isolated TC were incubated in 200 mM KCl, 10 mM HEPES, pH 7.4, 100 $\mu$M $Ca^{2+}$ or 100 $\mu$M EGTA, 20 nM ryanodine, 0.1 mM PMSF, and 1 $\mu$g/mL leupeptin (binding buffer) in the presence of increasing concentrations of S100A1 for 120 min at 37 °C. At the end of the incubation the samples were filtered on Whatman GF/B filters and washed with 50 volumes of ice-cold 200 mM KCl, 10 mM HEPES, pH 7.4; the amount of bound [$^3$H]ryanodine was determined by liquid scintillation counting. Unspecific binding was determined by incubating vesicles in the presence of an excess (100 $\mu$M) of cold ryanodine. Before use, S100A1 was incubated for 120 min in the presence of 1 mM EGTA and 10 mM DTT, and then dialyzed against 10 mM Tris-HCl, pH 7.5, in a cold room for 14−16 h.

*RYR $Ca^{2+}$ Channel Reconstitution and Single Channel Recording Analysis*. Lipid bilayers were cast from a phospholipid solution in *n*-decane containing a 5:2:3 mixture of phosphatidylethanolamine/phosphatidylserine/phosphatidylcholine (30 mg/mL). The voltage control side was the *cis* chamber, and the *trans* chamber was referred to as ground. Purified rabbit skeletal muscle $Ca^{2+}$ release channels (ryanodine receptor) were applied on top of the preformed bilayer from the *cis* side. The experimental solutions were as follows: for the *cis* chamber (mM), 250 NaCl, 10 HEPES, 0.1 $CaCl_2$, 0.1 EGTA (pH 7.0, pCa 5.52); for the *trans* chamber (mM), 50 NaCl, 10 HEPES, 0.1 $CaCl_2$, 0.1 EGTA (pH 7.4, pCa 5.52). Variations to these solutions are indicated in the legend to Figure 3. Free calcium concentrations were calculated according to the Chelator program (*24*). Data were acquired on-line at 200 $\mu$s/point (Axon Instruments) and filtered at 1 kHz using a low-pass Bessel filter. Single channel analysis was performed using the Transit program (A. M. J. Van Dongen, Department of Pharmacology, Duke University). The normalized $P_o$ was obtained from the ratio between the current integral and the maximum current integral.

*Affinity Chromatography*. The interaction between rabbit skeletal muscle RYR and S100A1 was investigated by affinity chromatography using Sepharose-conjugated S100A1.

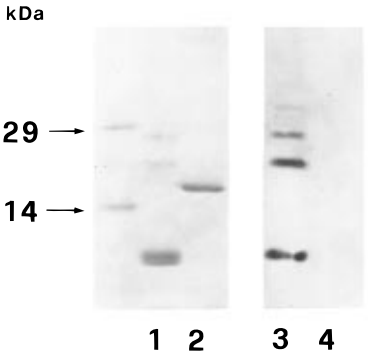


FIGURE 1: Purity of bovine brain S100A1. Two micrograms of purified S100A1 (lanes 1 and 3) and calmodulin (lanes 2 and 4) was loaded on a SDS−PAGE, and proteins were visualized by Coomassie BB staining (lanes 1 and 2, respectively). Lanes 3 and 4 are indirect immunoenzymatic staining of Western blots with anti-S100A1 Ab.

Briefly, after extensively washing the resin, 50 $\mu$L of resin was equilibrated with 50 mM Tris-HCl, pH 8.5, 150 mM NaCl, 0.1% CHAPS, and 1 mM EGTA and incubated with approximately 0.5−0.7 $\mu$g of purified RYR in the presence or absence of 1−5 $\mu$g of fusion proteins PC15, PC21, and PC27, overnight at 4 °C. The RYR fusion proteins were purified by electroelution from an SDS−polyacrylamide gel. The resin was washed with 10 bed volumes of the equilibration buffer, and the bound proteins were eluted with Laemmli solubilization buffer at 90 °C, 5 min. Proteins were run on a 7.5% SDS−PAGE and visualized by silver staining. Alternatively, two unrelated proteins were incubated overnight at 4 °C with S100A1-coupled Sepharose. The next day the resin was washed as described above for the RYR; proteins were separated by SDS−PAGE and visualized by silver staining.

## RESULTS

*Effect of S100A1 on [$^3$H]Ryanodine Binding to Isolated Terminal Cisternae*. Since S100A1 is abundant in skeletal muscle (ranging between 1 $\mu$g/mg of protein in human skeletal muscle and 292 ng/mg of rat skeletal muscle) (*25*, *14*) and has been shown to affect $Ca^{2+}$-induced $Ca^{2+}$ release, we investigated the effect of increasing concentrations of S100A1 on ryanodine binding to isolated rabbit skeletal muscle terminal cisternae. The S100A1 preparation we used throughout the experiments contains a major band of approximately 10 kDa (Figure 1, lane 1). In addition, there are protein components of higher molecular mass which represent S100A1 aggregates (dimers and, to a lower extent, trimers) as indicated by indirect immunoenzymatic staining with anti-S100A1 Ab (compare lanes 1 and 3). Figure 1 also shows that the S100A1 preparation is not contaminated by calmodulin since we could not detect a protein band corresponding to calmodulin in the S100A1 preparation (compare lanes 1 and 2). Equilibrium [$^3$H]ryanodine binding to the terminal cisternae fraction was first measured at optimal free [$Ca^{2+}$] (100 $\mu$M). Under these conditions, we could not determine any significant effect of S100A1 on the ryanodine binding activity. Thus, we investigated the effect at nanomolar free [$Ca^{2+}$]. As shown in Figure 2A, under these conditions S100A1 stimulated [$^3$H]ryanodine binding by 40 ± 6.7% (mean ± SE, $n = 5$) in a dose-dependent manner; the half-maximal concentration for stimulation of [$^3$H]ryanodine binding was 70 nM. We also measured [$^3$H]-ryanodine binding in the presence of 100 $\mu$M EGTA and 100 nM S100A1 at increasing concentrations of ryanodine. Scatchard plots (Figure 2B,C) constructed from our binding measurements show that S100A1 increases the apparent affinity of the receptor for [$^3$H]ryanodine ($K_d$ = 191 vs 383 nM in the presence and in the absence of S100A1, respectively). The $B_{max}$ values in the absence and in the presence of 100 nM S100A1 were 13.9 and 10.22 pmol/mg of TC, respectively. The effect of S100A1 on $B_{max}$ could result from an unstable equilibrium, which in turn leads to a decrease in receptor occupancy.

*Effect of S100A1 on the Single Channel Gating Properties of the Purifed RYR*. To determine if the interaction of S100A1 and ryanodine receptor resulted in a modification of channel function, we performed experiments on planar lipid bilayers using $Na^+$ as current carrier. Figure 3 shows the current integral and single channel recordings during sequential additions of calcium, EGTA, S100A1, and ruthenium red to the *cis* side of a planar lipid bilayer after incorporation of the purified RYR. At 3 $\mu$M free [$Ca^{2+}$], the normalized open probability was 0.17 and decreased after addition of EGTA to both sides of the membrane (free [$Ca^{2+}$] = 20 nM). Addition of S100A1 to the *cis* chamber induced a 6.0 ± 2.8-fold (mean ± SE, $n = 3$) increase of the normalized $P_o$ of the RYR channel blocked by EGTA. As expected, the S100A1-activated RYR channel could still be blocked by 12 $\mu$M ruthenium red (Figure 3). A further control was performed on the phospholipid membrane. In the presence of 800 nM S100A1 on both sides, the electrical properties of the bilayer were not affected (data not shown).

*S100A1 Binding Proteins of the Terminal Cisternae Fraction*. In order to identify S100A1 binding proteins present in terminal cisternae membranes, we carried out ligand overlay experiments. Thus, S100A1 was labeled with digoxigenin and used as a probe on ligand overlays of Western blots of either the terminal cisternae fraction or the insoluble fraction obtained after Triton X-100 treatment of terminal cisternae (junctional face membrane) (Figure 4). Our results show that in the terminal cisternae of rabbit skeletal muscle there are three major S100A1 binding proteins, having molecular masses of 565, 100, and 60 kDa (Figure 4, lane 4); these proteins are present in the insoluble fraction following treatment of terminal cisternae with Triton X-100 (Figure 4, lanes 3 and 6). Binding of S100A1 occurred to a similar extent at millimolar [$Ca^{2+}$] (Figure 4) and at nanomolar free [$Ca^{2+}$] (not shown). The labeled protein of 565 kDa represents the RYR protomer. We did not investigate in any further detail the other S100A1 binding proteins associated with the junctional face membrane.

The molecular interaction between S100A1 and the rabbit skeletal muscle RYR was also followed by biosensor measurements. Figure 5 shows the sensogram representing the real time interaction between sucrose gradient-purified RYR and the S100A1 immobilized on the sensor chip. The interaction between the purified RYR and S100A1 (i) occurred in the presence of millimolar free $Ca^{2+}$ concentrations (panel a, sensogram traces A, B, and C) and nanomolar [$Ca^{2+}$] (panel b, trace D), (ii) is dose-dependent (panel a), and (iii) could be inhibited by preincubation of the RYR with an excess of S100A1 (panel b, traces E and F). Interestingly, in the presence of millimolar $Ca^{2+}$, the rate of

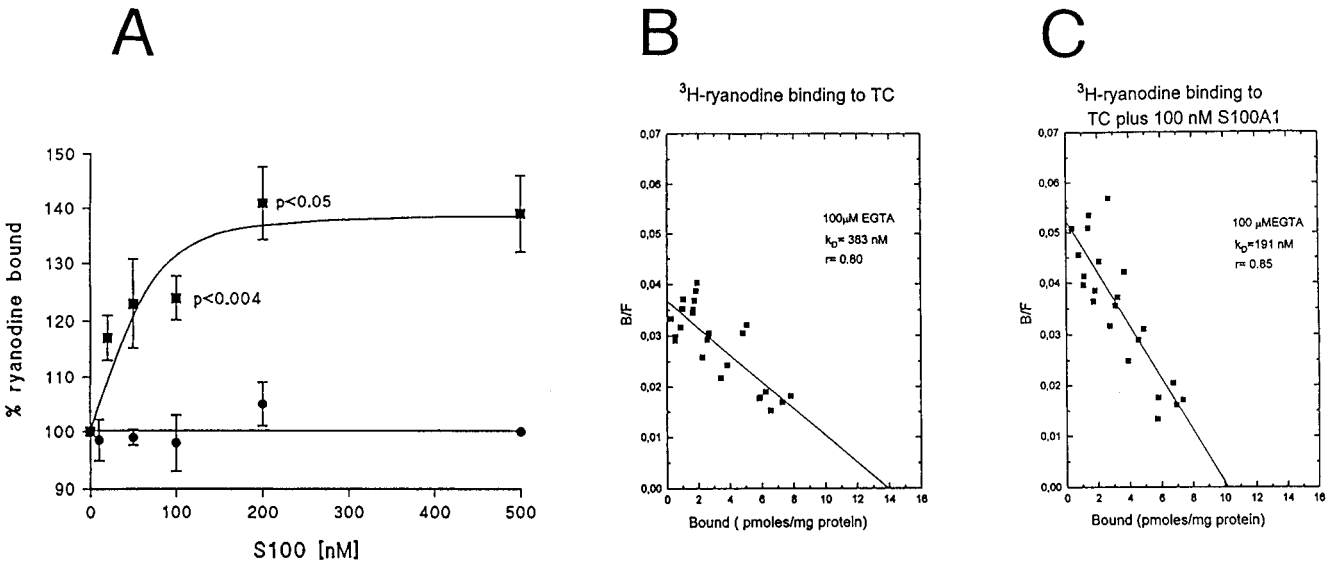


FIGURE 2: Effects of S100A1 on [$^3$H]ryanodine binding to terminal cisternae in the presence of nanomolar $Ca^{2+}$. Panel A: Rabbit terminal cisternae (60 $\mu$g) were incubated in the presence of increasing concentrations of S100A1 for 120 min at 37 °C, in the presence of 100 $\mu$M (filled circles) or 10 nM free $Ca^{2+}$ (filled squares). The amount of bound [$^3$H]ryanodine was determined as described under Materials and Methods. The results are expressed as percent mean (±SEM; $n = 5$) bound [$^3$H]ryanodine; 100% binding was that obtained in the absence of added S100A1 ($5.7 \pm 1.2$ and $1.4 \pm 0.54$ pmol of ryanodine bound/mg of protein in 100 $\mu$M free $Ca^{2+}$ and 10 nM free $Ca^{2+}$, respectively). Panels B and C: Scatchard analysis of [$^3$H]ryanodine binding to terminal cisternae in the absence (panel B) and presence (panel C) of S100A1. Seventy-five micrograms of terminal cisternae was incubated with [$^3$H]ryanodine over a concentration range of 7.5−450 nM ryanodine in the presence of 100 nM S100A1 and 100 $\mu$M EGTA as described under the Materials and Methods. Points represent duplicate determinations of four experiments carried out with two different terminal cisternae preparations.

interaction between the RYR and S100A1 was slightly more rapid than in the presence of nanomolar calcium [compare traces B and D; apparent association rates were $(6.2 \times 10^{-3}) + (1.5 \times 10^{-5})$ vs $(1.8 \times 10^{-3}) \pm (7.21 \times 10^{-6})$ $s^{-1}$ (mean ± SE), respectively]. Similarly, if the RYR was allowed to associate with S100A1 in the presence of millimolar $Ca^{2+}$, it dissociated from the latter protein more rapidly than when the two proteins had been allowed to interact in nanomolar [$Ca^{2+}$]. In the presence of EGTA, the equilibrium affinity of the RYR for the S100A1 immobilized on the sensor chip was $214 \pm 50$ nM, a value slightly higher than that observed when the interaction between RYR and S100A1 occurred in solution (Figure 2A). This result may be accounted for by the different experimental conditions used to measure the affinity. The signal generated by the S100A1-conjugated sensor chip could be due to the interaction between S100A1 and minor protein components which may contaminate the purified RYR preparation. In order to clearly identify the protein interacting with immobilized S100A1, we injected antibodies directed against the C-terminal region of RYR (*15*) in the flow cell after the interaction of the purified RYR preparation with the S100A1-conjugated sensor chip. Panel c shows the real time interaction of anti-RYR Ab with the RYR complex immobilized by S100A1 on the sensor chip, and unambiguously indicates the formation of a molecular complex between S100A1 and the RYR.

*Molecular Mapping of S100A1 Binding Sites.* In the next set of experiments, we mapped the RYR domain involved in the interaction with S100A1. Several fusion proteins covering the entire coding sequence of the rabbit skeletal muscle RYR were produced and assessed for their capacity to interact with digoxigenin-labeled S100A1 (Figure 6). As revealed by the overlay procedure, RYR fusion proteins PC21, PC15, and PC27 bound S100A1; however, the interaction of the different fusion proteins with their ligand occurred to different extents depending on the experimental conditions. Binding of S100A1 to PC21 occurred in the presence of both millimolar $Ca^{2+}$ (Figure 6B, lane 21b) and nanomolar free [$Ca^{2+}$] (Figure 6, lane 21c). On the other hand, binding to fusion protein PC27 was dependent on the presence of $Ca^{2+}$ (Figure 6B, compare lanes 27 b,c). In the presence of millimolar $Ca^{2+}$, S100A1 bound to a much lower extent to PC15 when compared to its binding activity at nanomolar [$Ca^{2+}$] (Figure 6B, lane 15c). The specificity of S100A1 binding to RYR fusion proteins was confirmed by incubating the blotted proteins in the presence of a 1000-fold excess of unlabeled protein (100 $\mu$M S100A1); as shown in Figure 7, binding to the RYR fusion proteins was abolished by the unlabeled protein. To define in further detail the S100A1 binding domain of PC21 and PC27, we carried out experiments with fusion proteins encompassing the $NH_2$-terminal portion of both fusion proteins. As can be seen in Figure 8, S100A1 binding to PC21 and PC27 requires the COOH-terminal region of both fusion proteins.

*Affinity Chromatography Using S100A1-Conjugated Sepharose.* We investigated the binding of purifed RYR complex to S100A1 by affinity chromatography using S100A1-conjugated Sepharose in the presence or absence of purified fusion proteins PC15, PC21, and PC27 (Figure 9). Purified RYR complex was incubated overnight with S100A1-conjugated Sepharose (panel A); alternatively, the S100A1-conjugated resin was preincubated for 30 min at room temperature with the electroeluted fusion proteins, followed by an overnight incubation with the purified RYR (panel B). The S100A1-conjugated Sepharose resin was then washed with 10 bed volumes of affinity chromatography buffer to remove the excess of RYR complex from the resin (Figure 9, panel A, lane B). RYR complex was associated with the S100A1-conjugated Sepharose resin as indicated by silver staining of eluting buffer (Figure 9, panel A, lane C). On the other hand, in the presence of competing polypeptides, binding of the purified RYR complex to the

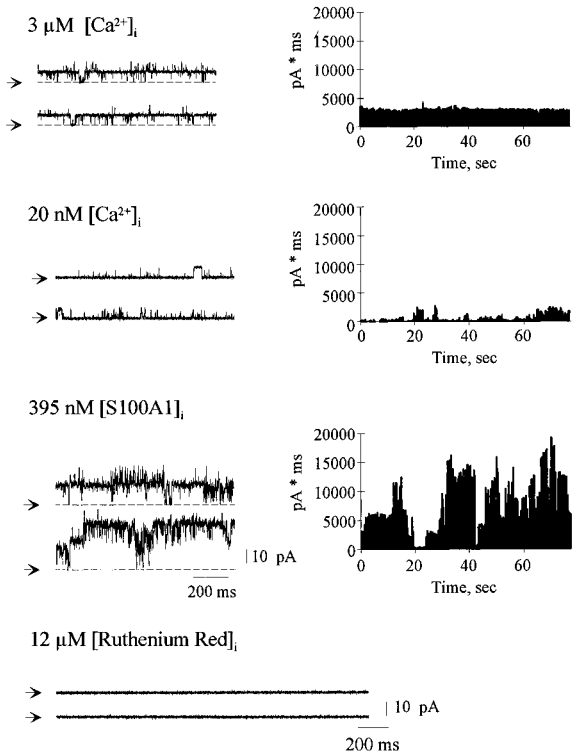


FIGURE 3: S100A1 activates the purified skeletal muscle $Ca^{2+}$ release channels (ryanodine receptor) incorporated into lipid bilayers. Current integral vs time plot and corresponding single channel recordings. Traces were recorded at 0 mV. Current integral values are 2998 pA*ms ($NP_o = 0.17$) in the control condition (3 $\mu$M free [$Ca^{2+}$]), 644 pA*ms ($NP_o = 0.036$) after addition of 400 $\mu$M EGTA (20 nM free [$Ca^{2+}$]), and 7434 pA*ms ($NP_o = 0.42$) after the addition of 395 nM S100A1 in the presence of nanomolar free [$Ca^{2+}$]. Ruthenium red completely blocked the reconstituted calcium release channel. Arrows indicate the closed state of the channel.

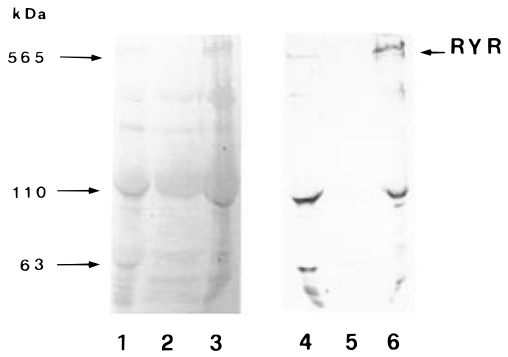


FIGURE 4: Identification of S100A1 binding proteins in rabbit skeletal muscle terminal cisternae and junctional face membrane. The proteins present in terminal cisternae (lanes 1 and 4) or in the supernatant (lanes 2 and 5) or pellet (lanes 3 and 6) after solubilization with Triton X-100 were separated on a 7.5% SDS−PAGE and blotted onto nitrocellulose (30 $\mu$g of protein/lane). Ligand overlay using digoxigenated S100A1. Lanes 1, 2, 3, Ponceau red staining of the Western blot; lanes 4, 5, 6, autoradiogram of the S100A1 overlay in the presence of 100 nM S100A1, 1 mM $Ca^{2+}$.

resin was abolished (Figure 9, panel B, lane C). We also examined whether unrelated purified proteins such as bovine serum albumin and carbonic anhydrase were able to bind to S100A1−sepharose resin. As can be seen in Figure 10, neither protein bound to the resin, indicating that the interaction between the RYR and S100A1-conjugated Sepharose is specific and requires the RYR sequences encompassed by fusion proteins PC15, PC21, and PC27.

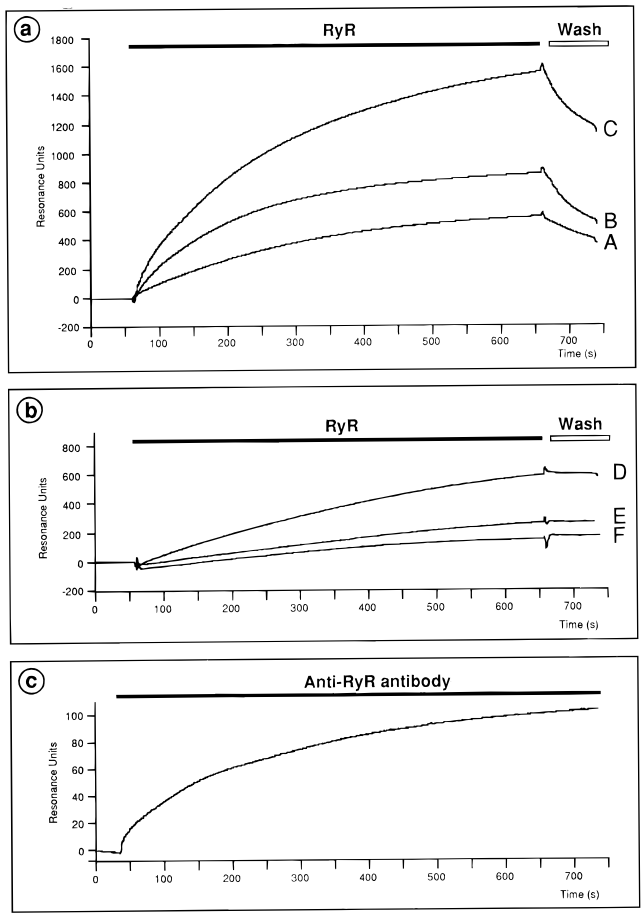


FIGURE 5: Characterization of the binding of purified RYR with S100A1 using surface plasmon resonance detection. S100A1 was immobilized on the CM5 sensor chip surface. Panel a: interaction of purified RYR with S100A1 in the presence of 2 mM $CaCl_2$. Curves are as follows: curve A, 3.4 $\mu$g of RYR; curve B, 7.25 $\mu$g of RYR; curve C, 10.8 $\mu$g of RYR. Panel b: interaction of purified RYR with S100A1 in the presence of 1 mM EGTA. Curves are as follows: curve D, 7.25 $\mu$g of RYR; curve E, 7.25 $\mu$g of RYR preincubated 10 min with 9.5 $\mu$g of S100A1; curve F, 7.25 $\mu$g of RYR preincubated 10 min with 19 $\mu$g of S100A1. The specific binding signal shown was obtained by subtracting the signal measured in the absence of immobilized S100A1 from the signal in the presence of immobilized S100A1. In the presence of $Ca^{2+}$ and EGTA, the unspecific signals were less than 10% and 20% of the total, respectively. Panel c: interaction of anti-RYR antibodies with the RYR-S100A1 complex. The purified RYR (6 $\mu$g) was first injected in the BIAsensor chip to which S100A1 had been coupled (see panel b). Antibodies (1/150 dilution) directed to the C-terminal region of the RYR were then injected. The specific binding signal was obtained by subtracting the signal measured in the absence of RYR from the signal measured in the presence of RYR. The unspecific signal in the absence of RYR was less than 30% of the total. The traces are representative of four different experiments.

## DISCUSSION

S100A1 is an EF-hand-type $Ca^{2+}$ binding protein which interacts with several protein targets, resulting in the modulation of a variety of cell functions including transduction of $Ca^{2+}$ signals, cytoskeletal interactions, cell cycle progression, and cell differentiation (see ref *10* and *9* for a review). The ryanodine receptor $Ca^{2+}$ channel has recently entered in the growing list of S100-modulated proteins. In fact, it has been shown that micromolar concentrations of S100A1 enhance $Ca^{2+}$-induced $Ca^{2+}$ release from the skeletal muscle terminal cisternae fraction via the ryanodine receptor calcium channel (*12*, *13*). Using a combination of biophysical and biochemi-

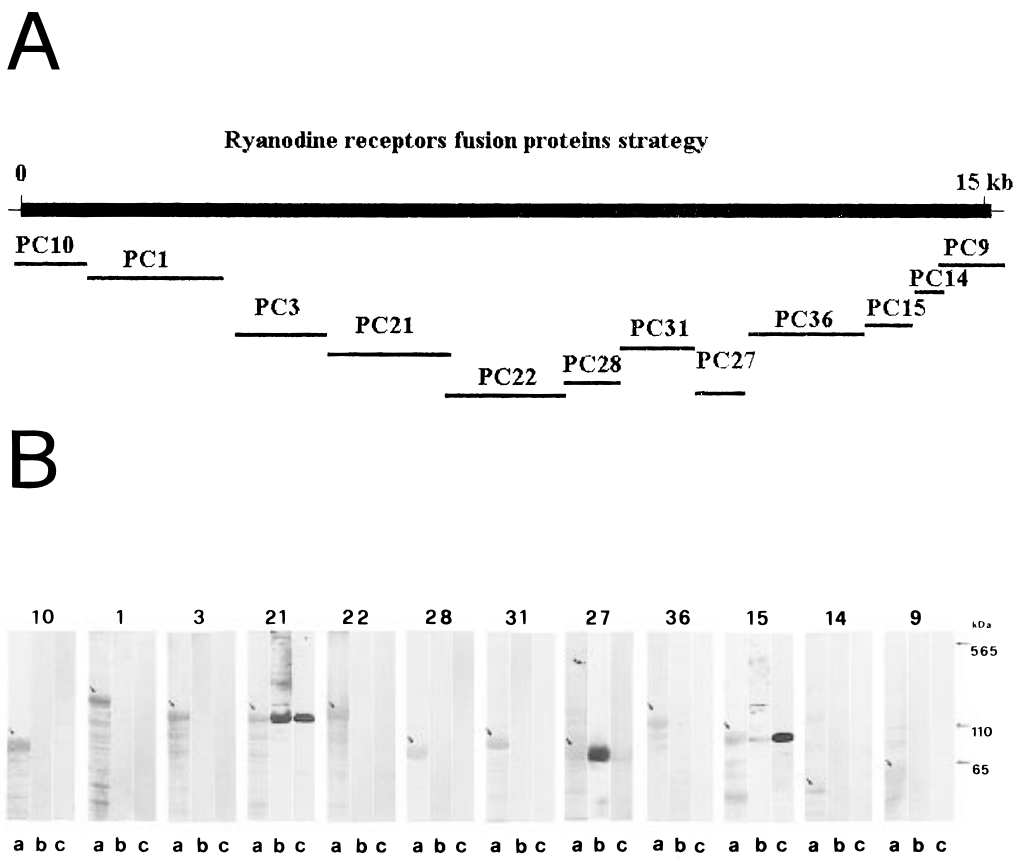


FIGURE 6: Identification of S100A1 binding sequences of the skeletal muscle RYR. Panel A: fusion protein production strategy. The top line indicates the size of the full-length rabbit RYR cDNA (Zorzato et al., 1990). The numbering is positive beginning at the first nucleotide of the initiator methionine. The underlying segments indicate the sizes of the cDNA fragments cloned into the pATH vectors. Panel B: S100A1 overlays. 20−50 $\mu$L of total *E. coli* extracts was electrophoretically separated in a 7.5% SDS−PAGE and transferred onto nitrocellulose. Lanes a, Ponceau red staining of the western blots; lanes b, autoradiogram of the overlays performed in the presence of 1 mM $Ca^{2+}$; lanes c, autoradiograms of the overlays performed in the presence of 1 mM EGTA. Arrows indicate the RYR fusion proteins.

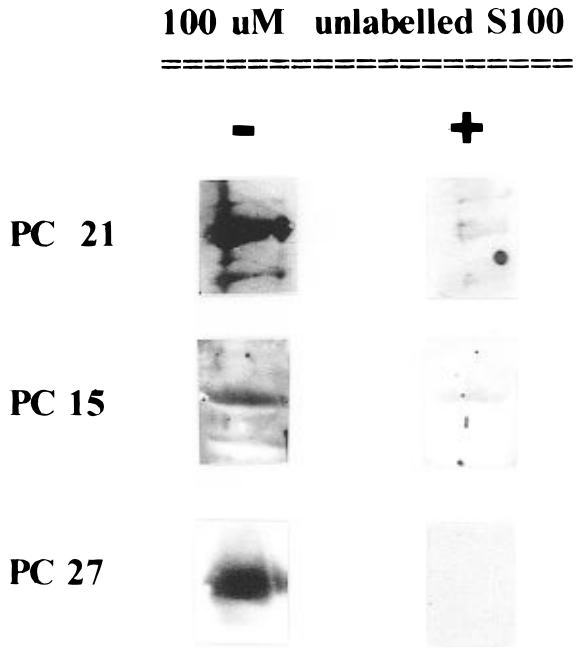


FIGURE 7: Binding of S100A1−digoxigenin to the fusion proteins PC21, PC15, and PC27 is specific. Proteins in bacterial extracts were separated in a 7.5% SDS−PAGE and transferred to nitrocellulose. The bands corresponding to the RYR fusion proteins were cut, and ligand overlays were performed in the absence (−) or presence (+) of a 1000-fold excess of unlabeled S100A1.

cal approaches we demonstrate that the skeletal muscle ryanodine receptor interacts directly with S100A1 and that such an interaction affects the functional state of the RYR. As to the RYR sequences involved in the binding of S100A1, our ligand overlay data indicate that there are at least three S100A1 binding domains defined by residues 1861−2155 (S100A1#1), 3774−3874 (S100A1#2), and 4425−4621 (S100A1#3), respectively. The specificity of the interaction between S100A1 and SDS-denatured RYR fusion proteins is confirmed by several experimental results: (1) S100A1 binds only to 3 fusion proteins out of 11 we tested; (2) binding can be competed by an excess of unlabeled S100A1; (3) partial sequence deletion of the S100A1 binding fusion protein eliminates binding activity; (4) binding does not occur randomly throughout the RYR protomer's sequence: (i) one domain (PC27) contains a consensus sequence for S100 binding (Figure 8, panel A); (ii) overlays with digoxigenin-labeled calmodulin, an EF-hand $Ca^{2+}$ binding protein having similar properties to S100A1, were positive with RYR sequences distinct from those labeled with S100A1 (*23*), the only exception being PC15 fusion protein. The latter fusion protein encompasses a low-affinity calmodulin binding site, and its labeling with S100A1 is not surprising since it has been shown that low-affinity calmodulin binding sites may overlap with S100 binding sites. S100A1 binding to RYR domains 1, 2, and 3 differs in $Ca^{2+}$ sensitivity: domain 1 binds the ligand in the presence of millimolar $Ca^{2+}$ and EGTA, domain 2 binds S100A1 in the presence of milimolar $Ca^{2+}$, and domain 3 displays either weak or strong binding activity in the presence of millimolar or nanomolar $Ca^{2+}$, respectively. With the entire RYR protomer, there is no

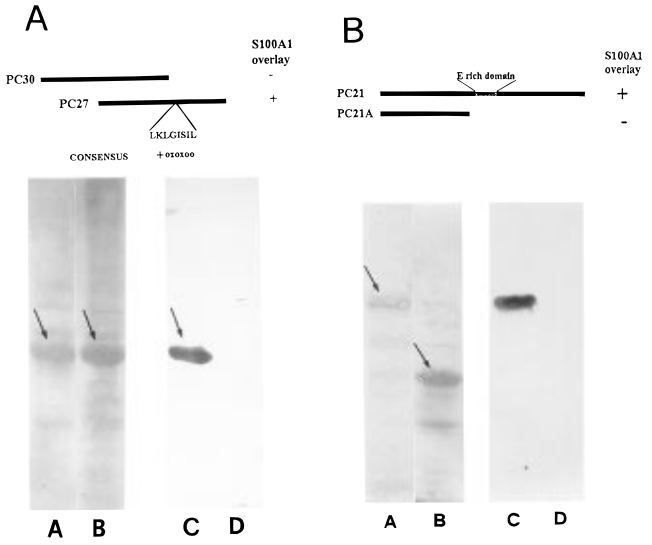


FIGURE 8: Identification of the domain of fusion proteins PC21 and PC27 involved in the interaction with S100A1. 20−50 $\mu$L of total *E. coli* extracts was electrophoretically separated in a 7.5% SDS−PAGE and transferred onto nitrocellulose. Lanes A and B, Ponceau red staining of the western blot. Arrows indicate the RYR fusion proteins. Lanes C and D, autoradiograms of the digoxigenin-labeled S100A1 overlays performed in the presence of 1 mM $Ca^{2+}$. Panel A: The upper part shows a schematic representation of the domain within PC27 involved in the interaction with S100A1. Lanes A and C, PC27; lanes B and D, PC30. The consensus sequence is indicated in the single-letter code: +, positively charged residues; o, hydrophobic residues; x, variable residues. Panel B: The upper part shows a schematic representation of the domains within PC21 involved in the interaction with S100A1. Lanes A and C, PC21; lanes B and D, PC21A carrying a deletion of the COOH terminus.

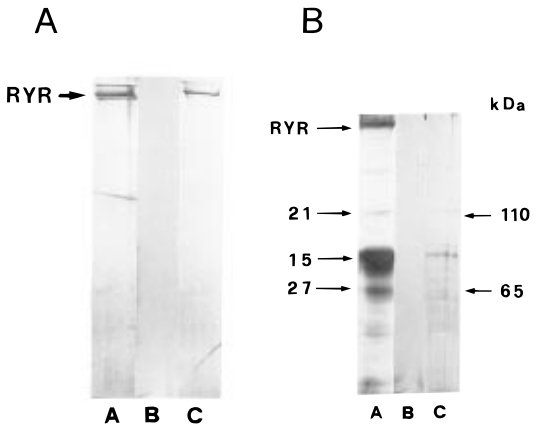


FIGURE 9: Affinity chromatography of the RYR on S100A1−Sepharose. Panel A: The purified RYR was incubated overnight at 4 °C with S100A1−Sepharose. The resin was washed with 10 bed volumes of 50 mM Tris-HCl, pH 8.5, 150 mM NaCl, 0.1% CHAPS, and 1 mM EGTA, and the bound proteins were eluted with Laemmli solubilization buffer. Panel B: Experimental conditions as in panel A except that the S100A1 resin was preincubated with the electroeluted fusion proteins PC21, PC15, and PC27 for 20 min before incubation with the purified RYR.

effect of $Ca^{2+}$ on S100A1 binding (Figure 4). This apparent discrepancy can be explained by the results with RYR fusion proteins. It is likely that overlays with the entire RYR protomer do not discriminate the contribution to the S100A1 binding activity of each domain at different [$Ca^{2+}$]. S100A1 domain 1 comprises the "glutamate rich" region and is localized in the central portion of the molecule (see Figure 8, panel B) within the $NH_2$ terminal of the receptor which has been predicted to form the large hydrophilic part of the

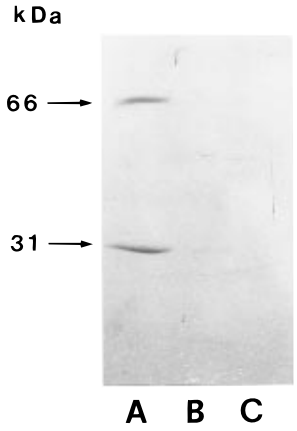


FIGURE 10: Interaction of purified RYR with S100A1−Sepharose is specific. Experimental conditions as in Figure 9 except that the S100A1 resin was incubated with bovine serum albumin and with bovine carbonic anhydrase (1 $\mu$g of each protein). Lane A, void volume; lane B, last wash; and lane C, addition of solubilization buffer. Proteins were separated on a 7.5% (lanes A and B) or 10% (lane C) SDS−PAGE and visualized by silver staining. Fifty microliters of each fraction was loaded per lane; left arrows indicate molecular mass markers.

RYR. According to the 12 transmembrane segment model of the RYR (*5*), S100A1 binding domain 2 is localized approximately 200 residues upstream of the putative transmembrane segment M1, while S100A1 binding domain 3 is close to the putative transmembrane segment M5. Interestingly, S100A1 domain 2 contains a consensus sequence for S100 binding proteins (Figure 6A) (*27*) which is highly conserved throughout evolution and among different RYR isoforms (*28*). The exact physiological relevance of these S100A1 binding sites is not fully established; however, we think that they could play a role in the regulation of the $Ca^{2+}$ release channel in skeletal muscle since S100A1 interacts with the ryanodine receptor at a concentration well below the estimated concentration of the former protein in striated muscle (*14*, *25*). Heart and skeletal muscles have been reported to contain 0.2−1 $\mu$g/mg of wet tissue of S100A1. Assuming that 1 g of wet muscle is equal to a fiber volume of 1 mL, the resulting total concentration of S100A1 in striated muscles would range between 50 and 100 $\mu$M, a value at least 500 times higher than that we used for the *in vitro* studies.

The most interesting and novel results obtained in the present study concern the ability of S100A1 to interact with RYR sequences in the presence of nanomolar free [$Ca^{2+}$]. Under these conditions, we observed S100A1 binding to domains 1 and 3. Such a result is consistent with the finding that few other S100 binding proteins, including glycogen phosphorylase and synthase, aldolase, myosin, and tau protein, interact with their ligands at low free [$Ca^{2+}$] (*27*). The interaction of S100A1 with the RYR at low free [$Ca^{2+}$] is associated with an enhancement of the equilibrium binding of [$^3$H]ryanodine to terminal cisternae. It is also clear that S100A1 enhances the activity of the purified RYR after incorporation in the bilayer because it causes a significant increase of the current integral. The purifed RYR displays four main subconductance states. It seems that the prevailing transition in the absence of S100A1 is from closed to half of its maximal conductance, while in the presence of S100A1 the prevailing transition is apparently from closed to maximal conductance level. S100A1 enhances the channel's opening;

thus, we cannot exclude the possibility that the higher conductance levels observed in the presence of S100A1 may also result from simultaneous opening of more than one channel present in the bilayer. The interaction and the effect of S100A1 on RYR at low free [$Ca^{2+}$] are reminiscent of those of calmodulin (*29*, *30*, *31*), since the latter EF-hand $Ca^{2+}$ binding protein also stimulates the RYR channel activity upon interaction with the receptor at nanomolar free [$Ca^{2+}$]. Ligand overlays and conventional calmodulin binding experiments have indicated that at free [$Ca^{2+}$] similar to those of resting muscle the RYR binds calmodulin (*23*, *32*, *29*, *31*) with a stoichiometry of 12/16 calmodulin molecules per RYR tetramer complex (*32*, *29*). Thus, under the same conditions, the RYR tetramer complex could also interact with eight S100A1 molecules. If this is the case, the RYRs of resting muscle could potentially interact with a total of 12−24 EF-hand-type $Ca^{2+}$ binding proteins. This is particularly relevant in view of the fact that (i) analysis of the primary structure of the RYR failed to identify a clear consensus sequence encompassing a high-affinity $Ca^{2+}$ binding site of the EF-hand type (*5*) and (ii) the $Ca^{2+}$-induced $Ca^{2+}$ release mechanism of the RYR operates at free [$Ca^{2+}$] ranging from nanomolar to micromolar (*33*). We propose that some of the EF-hand type $Ca^{2+}$ binding proteins which interact with the RYR at [$Ca^{2+}$] similar to those of resting muscle may act as $Ca^{2+}$ sensors of the $Ca^{2+}$-induced $Ca^{2+}$ release mechanism. Thus, according to such a model, conformational changes induced by $Ca^{2+}$ binding to the high affinity binding sites of the EF-hand type $Ca^{2+}$ binding proteins are transmitted to the channel and elicit its opening.

Interestingly, the RYR polypeptide defined by residues 4425−4621 (PC15 fusion protein) encompasses an S100A1 binding domain and a low-affinity calmodulin binding domain. This region has already been implicated in the $Ca^{2+}$−dependent regulation of the $Ca^{2+}$ release channel. In fact, it has been shown that polyclonal Ab against a polypeptide encompassing PC15 can both block and enhance the RYR channel activity (*34*, *35*, *36*, *22*, *37*). Though the "blocking" and "enhancing" effects may seem at first contradictory, the former consequence may be due to the perturbation of CaM binding domain 3, while the enhancing effect would result from a perturbation of the S100A1 binding domain 3. If this proves to be so, the interaction of the EF-hand $Ca^{2+}$ binding proteins with the region defined by residues 4425−4621 might be crucial for the $Ca^{2+}$-dependent regulation of the native RYR channel complex.

## REFERENCES


1. Coronado, R., Morissette, J., Sukhareva, V., and Vaughan, D. M. (1994) *Am. J. Physiol*. C1485−C1504.
2. Meissner, G. (1994) *Annu. Rev. Physiol. 56*, 485−508.
3. Sutko, J. L., and Airey, J. A. (1996) *Physiol. Rev. 76*, 1027−1071.
4. Takeshima, H., Nishimura, S., Matsumoto, H., Ishida, K., Kangawa, N., Minamino, H., Matsuo, M., Ueda, M., Hanakoa, M., Hirose, T., and Numa, S. (1989) *Nature 339*, 439−445.
5. Zorzato, F., Fujii, J., Otsu, K., Phillips, M., Green, N. M., Lai, F. A., Meissner, G., and MacLennan, D. H. (1990) *J. Biol. Chem. 265*, 2244−2256.
6. Nakai, J., Imagawa, T., Hakamata, Y., Shigekawa, M., Takeshima, H., and Numa, S. (1990) *FEBS Lett. 271*, 169−177.
7. Hakamata, Y., Nakai, J., Takeshima, H., and Imoto, K. (1992) *FEBS Lett. 312*, 229−235.
8. Jayaraman, T., Brillantes, A. M., Timmerman, A. P., Fleischer, S., Erdjument-Bromgel, H., Tempst, P., and Marks, A. R. (1992) *J. Biol. Chem. 267*, 9474−9477.
9. Schafer, B. W., and Heizmann, C. W. (1996) *Trends Biochem. Sci. 21*, 134−140.
10. Klingman, D., and Hilt, D. C. (1988) *Trends Biochem. Sci. 13*, 437−443.
11. Baudier, J., Mochly-Rosen, D., Newton, A., Lee, S. H., Koshland, D. E., and Cole, R. D. (1987) *Biochemistry 26*, 2886−2893.
12. Fano', G., Marsili, V., Angela, P., Aisa, M. C., Giambianco, I., and Donato R. (1990) *FEBS Lett. 255*, 381−384.
13. Marsili, V., Mancinelli, L., Menchetti, G., Fulle, S., Baldoni, F., and Fano', G. (1992) *J. Muscle Res. Cell Motil. 13*, 511−515.
14. Kato, K., Kimura, S., Haimoto, H., and Suzuki, F. (1986) *J. Neurochem. 46*, 1555−1560.
15. Marty, I., Villaz, M., Arlaud, G., Bally, I., and Ronjat, M. (1994) *Biochem. J. 298*, 743−749.
16. Saito, A., Seiler, S., Chu, A., and Fleischer, S. (1984) *J. Cell Biol. 99*, 975−985.
17. Lowry, O. H., Rosenbrough, N. J., Farr, A. L., and Randal, R. J. (1951) *J. Biol. Chem. 193*, 265−275.
18. Costello, B., Chadwick, C., Saito, A., Chu, A., Maurer, A., and Fleischer, S. (1986) *J. Cell Biol. 103*, 741−753.
19. Lai, F. A., Erickson, H. P., Rousseau, E., Liu, Q. Y., and Meissner, G. (1988) *Nature 331*, 315−319.
20. Zorzato, F., Menegazzi, P., Treves, S., and Ronjat, M. (1966) *J. Biol. Chem. 271*, 22759−22763.
21. Maniatis, T., Fritsch, E. F., and Sambrook, J. (1989). *Molecular Cloning: A Laboratory Manual*, Second ed., Cold Spring Harbor Laboratory, Cold Spring Harbor, NY.
22. Treves, S., Chiozzi, P., and Zorzato, F. (1993) *Biochem. J. 291*, 757−763.
23. Menegazzi, P., Larini, F., Treves, S., Guerrini, R., Quadroni, M., and Zorzato, F. (1994) *Biochemistry 33*, 9078−9084
24. Schoenmakers, T. J. M., Visser, G. J., Flick, G., and Theuvenet, A. P. R. (1992) *BioTechniques 12*, 870.
25. Kato, K., and Kimura, S. (1985) *Biochim. Biophys. Acta 842*, 146−150.
26. Mely, Y., and Gerard D. (1990) *J. Neurochem. 55*, 1100−1106.
27. Ivankenov, V. V., Jamieson, G. A., Gruenstein, E., and Dimlich, R. V. W. (1995) *J. Biol. Chem. 270*, 14651−14658.
28. Oyamada, H., Murayama, T., Takagi, T., Iino, M., Iwabe, N., Miyata, T., Ogawa, Y., and Endo, M. (1994) *J. Biol. Chem. 269*, 17206−17214.
29. Tripathy, A., Xu, L., Mann, G., and Meissner, G. (1995) *Biophys. J. 69*, 106−119.
30. Buratti, R., Prestipino, G., Menegazzi, P., Treves, S., and Zorzato, F. (1995) *Biochem. Biophys. Res. Commun. 213*, 1082−1090.
31. O'Driscoll, S., McCharthy, T. M., Eichinger, H. M., Erhardt, W., Lehmann-Horn, F., and Herrmann-Frank, A. (1996) *Biochem. J. 319*, 421−426.
32. Yang, H., Reedy, M. M., Burke, C. L., and Strasburg, G. M. (1994) *Biochemistry 33*, 518−525.
33. Rios, E., and Pizarro, G. (1991) *Physiol. Rev 71*, 849−907.
34. Zorzato, F., Chu, A., and Volpe, P. (1989) *Biochem. J. 261*, 863−870.
35. Fill, M., Mejia-Alvarez, R., Zorzato, F., Volpe, P., and Stefani, E. (1991) *Biochem. J. 273*, 449−457.
36. Chen, S. R. W., Zhang, L., and MacLennan, D. H. (1992) *J. Biol. Chem. 267*, 23318−23326.
37. Chen, S. R. W., Zhang, L., and MacLennan, D. H. (1993) *J. Biol. Chem. 267*, 23318−23326.


BI970160W